



Search for Standard Model Higgs Boson Production in Association with a W^\pm Boson with 7.5 fb^{-1} of CDF Data

The CDF Collaboration
URL <http://www-cdf.fnal.gov>
(Dated: July 18, 2011)

We present a search for the standard model Higgs boson produced in association with a W^\pm boson. This search uses data corresponding to an integrated luminosity of 7.5 fb^{-1} collected by the CDF detector at the Tevatron. We select $WH \rightarrow \ell\nu b\bar{b}$ candidate events with two jets, large missing transverse energy, and exactly one charged lepton from the central or forward regions of the detector. We further require that at least one jet be identified to originate from a bottom quark. Discrimination between the Higgs boson signal and the comparatively large backgrounds is improved through the use of a Bayesian artificial neural network. The number of tagged events and the resulting neural network output distributions are consistent with the standard model expectations. We observe no evidence for a Higgs boson signal and set 95% confidence level upper limits on the WH production cross section times the branching ratio to decay to $b\bar{b}$ pairs, $\sigma(p\bar{p} \rightarrow W^\pm H) \times BR(H \rightarrow b\bar{b})$. For the mass range of $100 \text{ GeV}/c^2$ through $150 \text{ GeV}/c^2$ we set observed (expected) upper limits from $1.34 (1.83) \times \text{SM}$ through $38.8 (23.4) \times \text{SM}$. For $115 \text{ GeV}/c^2$ the upper limit is $3.64 (2.78)$. When we combine this search with an independent analysis that selects events with 3 jets, we set limits in the same mass range from $1.12 (1.79) \times \text{SM}$ through $34.4 (21.6) \times \text{SM}$ and for $115 \text{ GeV}/c^2$ the upper limit is $2.65 (2.60)$.

I. INTRODUCTION

The Higgs boson is the only elementary particle predicted by the standard model (SM) of elementary particles and their interactions that has not been either confirmed nor ruled out by experiments. It is predicted by the Higgs mechanism in order to explain the spontaneous symmetry breaking and the origin of mass for the electroweak gauge bosons and the fermions. If the Higgs boson is observed experimentally, it will confirm the SM and the Higgs mechanism. If it is confirmed not to exist, another model will have to be identified to describe correctly the spontaneous symmetry breaking in nature.

We perform a search for the SM Higgs boson using data collected by the Collider Detector at Fermilab at the Tevatron with an integrated luminosity of 7.5 fb^{-1} . Direct searches at the LEP and Tevatron accelerators, as well as indirect electroweak fits, have constrained the Higgs boson mass at 95% confidence level in the ranges [114.4-158] and [175-185] GeV/c^2 [1, 2]. Since the preferred mass for electroweak fits is in the former interval, we choose to perform a search for low Higgs boson masses. For low Higgs boson masses (below $135 \text{ GeV}/c^2$), the dominant decay mode is $H \rightarrow b\bar{b}$. The dominant production mode at the Tevatron is gluon fusion producing one Higgs boson and nothing else. Since the desired Higgs boson decays to a bottom-antibottom quark pair, the signal could not be distinguished from the SM bottom quark pair production, which is 9 orders of magnitude higher. For this reason, we consider the next most abundant Higgs production mechanism at the Tevatron, namely the associated production of a Higgs boson with a W boson, also called Higgsstrahlung, since a virtual W boson radiates a Higgs boson [3]. In this analysis, we select $WH \rightarrow \ell\nu b\bar{b}$ candidate events with a charged lepton, missing transverse energy and two jets originating from bottom quarks. The selection of a charged lepton reduces greatly the background fraction in the sample. We also include the signal contribution of $ZH \rightarrow \ell\ell b\bar{b}$, where one of the charged leptons escapes detection, which adds about 3% more signal. We use complementary high- p_T lepton and missing transverse energy (\cancel{E}_T) triggers to maximize our signal acceptance.

The latest WH search from CDF [4] was performed using a dataset with an integrated luminosity of 5.7 fb^{-1} , which is 24% smaller than the current analysis dataset. Just as in the latest analysis, the current analysis employs a Bayesian artificial neural network (BNN) discriminant [5] to improve discrimination between signal and background. However, the current analysis embodies improvements. The signal acceptance is improved in the loose charged lepton categories by using an additional trigger based on jets and missing transverse energy, as well as a novel method to combine any number of triggers in order to maximize the event yield and yet avoid correlations between triggers. Also, the signal acceptance is increased by using different loose lepton reconstruction algorithms, for loose muon and loose electron candidates. In addition, the fraction of events where pure non- W boson (QCD) events are faking a W boson is diminished by using a more sophisticated algorithm based on a Support Vector Machine [6] technique for most of the considered lepton categories. This allows us to reduce the \cancel{E}_T cut for some charged lepton categories as well, thus increasing the signal acceptance further.

II. DATA SAMPLE & EVENT SELECTION

A. Triggers

We use lepton, $\cancel{E}_T + \text{jets}$, and \cancel{E}_T triggered data collected through March 2011 and corresponding to an integrated luminosity of 7.5 fb^{-1} . The events are collected by the CDF II detector and classified according to their trigger type.

Central lepton events enter the analysis from high- p_T electron or muon triggers that have an 18 GeV threshold [7]. Some candidates that fail the standard electron reconstruction are recovered if they are deemed to be electron-like according to a multivariate likelihood method (loose electron-like leptons). The electron or muon is further required offline to be isolated with E_T (or p_T) $> 20 \text{ GeV}$ (GeV/c). Since the W +jets signature presents a large missing transverse energy, we require $\cancel{E}_T > 20 \text{ GeV}$ ($\cancel{E}_T > 10 \text{ GeV}$) for electrons (muons).

We select forward (plug) electron events with a trigger intended for W candidate events. The plug electron trigger requires both a plug electron candidate and missing transverse energy. Plug electron events are further required offline to have $E_T > 20 \text{ GeV}$ and $\cancel{E}_T > 25 \text{ GeV}$.

We select $\cancel{E}_T + \text{jet}$ and \cancel{E}_T triggered events that have an identified loose (non-triggered) lepton. The efficiency of

the different triggers is parametrized using sigmoid turn-on curves in \cancel{E}_T , without correcting for the muon momenta. For each event, only the most efficient trigger is considered. The \cancel{E}_T trigger requires 45 GeV of uncorrected missing transverse energy. Two \cancel{E}_T + jet triggers are used and tight offline cuts are imposed: two jets with $E_T > 25$ GeV, $\Delta R > 1.0$, and at least one central jet with $|\eta| < 0.9$ are required in one case, while in the other the presence of two jets with $E_T > 40$ and $E_T > 25$ GeV is required.

B. Event Selection

We consider different muon types of non-triggered leptons that are primary from the $W \rightarrow \mu\nu$ decay where the muon failed the standard identification or entered into a detector gap region. Some of these lepton candidates are taken from the extended muon coverage (EMC) [8]. Isolated tracks that have $p_T > 20$ GeV, are isolated from other track activity in the event, and that do not belong to any of the EMC categories are also selected and included in the category of non-triggered muons. Isolated tracks with significant deposits of energy in the calorimeter are also selected and included in the category of loose electron-like leptons. These lepton candidates originate primarily from the leptonic decay of the W boson, where the electron fails the standard identification, or the τ lepton decays in a single charged hadron (one-prong). Only one \cancel{E}_T + jet and the \cancel{E}_T triggers are used to select these events. A simplified procedure to decide which of the two triggers is considered for each event is used for this lepton category.

We increase the purity of the sample by applying cuts intended to remove fake events from QCD processes. The QCD veto is based on a Support Vector Machine [6] that uses different kinematical input variables. Some of them are related to the W kinematics like the lepton p_T , \cancel{E}_T , or $\Delta\phi(\text{lepton}, \cancel{E}_T^{\text{uncorrected}})$. Some are related to the kinematics of the jets in the event like $\cancel{E}_T^{\text{uncorrected}}$ and the transverse energy of the second leading E_T jet. A variable denoted as \cancel{E}_T significance is also used. This variable is defined as the ratio of \cancel{E}_T to a weighted sum of factors correlated with mismeasurement, such as angles between the \cancel{E}_T and the jets and the amount of jet energy corrections.

For forward electrons and loose electron-like leptons a cut based QCD veto is used. This veto applies a linear cut on the \cancel{E}_T and the azimuthal angle (ϕ) between the \cancel{E}_T and each of the jets ($E_T > 45 - (30 \cdot |\Delta\phi|)$), requires a large transverse mass of the reconstructed W ($M_T(W) > 20$ GeV), and a large \cancel{E}_T significance.

The events from all trigger types are classified according to the number of jets having $E_T > 20$ GeV and $|\eta| < 2.0$. Events that have exactly two jets are selected, while events with a different number of jets are used as control regions. Because the Higgs boson decays to $b\bar{b}$ pairs, we employ b -tagging algorithms that rely on the relatively long lifetime and large mass of the b quark. We require at least one of the jets in the event to be b -tagged by a secondary vertex tagging algorithm (denoted as SecVtx). Other b -tagging algorithms are considered (more details are given in the next section). For events with one SecVtx tagged jet and one other jet that is not tagged by any of the other considered b -tagging algorithms, we reduce the contamination from events with a fake W boson by applying the previously described QCD veto.

C. Bottom Quark Tagging Algorithms

To reduce considerably the backgrounds to this Higgs boson search, we require that at least one jet in the event be identified as originating from a b quark by the SecVtx algorithm. The secondary vertex tagging algorithm identifies b quarks by fitting tracks displaced from the primary vertex. This method has been used in other Higgs boson searches and in studies of top-quark properties [9]. In addition, we use the jet probability tagging algorithm, which identifies b quarks by requiring a low probability that all tracks contained in a jet originated from the primary vertex, based on the track impact parameters [10]. We also use a neural-network-based tagging algorithm that identifies b quarks by combining the information about displaced vertices, displaced tracks and low p_T muons. We use four mutually exclusive tagging categories: two SecVtx tags (ST+ST), one secondary vertex tag and one jet probability tag (ST+JP), one secondary vertex tag and one neural network tag (ST+NN) and exactly one SecVtx tag (1-ST).

D. Total WH (ZH) Acceptance

The signal acceptance is measured in a sample of Monte Carlo events generated with the PYTHIA program [11]. We consider the signal acceptance not only from the $WH \rightarrow \ell\nu b\bar{b}$ process, but also from $ZH \rightarrow \ell\ell b\bar{b}$, with one undetected lepton. The detection efficiency for the signal events is defined as

$$\epsilon_{WH(ZH)\rightarrow\ell\nu b\bar{b}} = \epsilon_{z_0} \cdot \epsilon_{\text{trig}} \cdot \epsilon_{\text{leptonid}} \cdot \epsilon_{WH(ZH)\rightarrow\ell\nu b\bar{b}}^{\text{MC}} \cdot \left(\sum_{\ell=e,\mu,\tau} Br(W \rightarrow \ell\nu(Z \rightarrow \ell\ell)) \right), \quad (1)$$

where $\epsilon_{WH(ZH)\rightarrow\ell\nu b\bar{b}}^{\text{MC}}$ is the fraction of signal events (with $|z_0| < 60$ cm) passing the kinematic requirements. The difference in b -tagging efficiency between data and MC is accounted for by applying scale factors for the different considered b -tagging algorithms to the MC. The quantity ϵ_{z_0} is the efficiency of the $|z_0| < 60$ cm cut, ϵ_{trig} is the trigger efficiency; $\epsilon_{\text{leptonid}}$ is the efficiency to identify a lepton; ϵ_{iso} is efficiency of the energy isolation cut; and $BR(W \rightarrow \ell\nu(Z \rightarrow \ell\ell))$ is the branching ratio for leptonic $W(Z)$ decay. For plug electrons, ϵ_{trig} is parameterized as a function of the trigger missing transverse energy and the E_T of the electron.

Table I shows the number of expected signal events for each tagging category at a Higgs boson mass of $115 \text{ GeV}/c^2$. Since the three categories of double-tagged events and one category of single-tagged events are defined exclusively, the total acceptance is given by the sum of the acceptance for the four categories.

$WH \rightarrow \ell\nu b\bar{b}$, 2 jets							
CDF Run II Preliminary 7.5 fb^{-1}							
Number of Expected WH and ZH Events at $M(H) = 115 \text{ GeV}/c^2$							
Tag	CEM	PHX	CMUP	CMX	NTM	LEL	All Leptons
ST+ST	2.40	0.36	1.38	0.71	1.69	0.74	7.28
ST+JP	1.73	0.25	1.03	0.53	1.25	0.55	5.34
ST+NN	0.92	0.14	0.53	0.27	0.64	0.30	2.80
1-ST	5.20	0.93	2.95	1.50	3.64	1.74	16.0
All Tags	10.3	1.68	5.89	3.01	7.22	3.33	31.4

TABLE I: Expected number of WH and ZH events for $M(H) = 115 \text{ GeV}/c^2$, shown for each tag category and lepton type. CEM makes reference to triggered central electrons that pass the standard reconstruction. PHX make reference to triggered forward electrons. CMUP and CMX make reference to triggered central muons detected with the corresponding muon detector. The NTM category makes reference to the different types of non-triggered muons. The LEL (loose electron-like leptons, described in Section II) category makes reference both to triggered electron-like leptons that fail the standard reconstruction but have a high multivariate likelihood value and to non-triggered ones reconstructed as isolated tracks matched to significant deposits of energy in the calorimeter.

III. BACKGROUNDS

This analysis builds on the method of background estimation detailed in Ref. [9]. In particular, the contributions from the following individual backgrounds are calculated: falsely b -tagged events, W production with heavy flavor quark pairs, QCD events with false W signatures, top quark production, and diboson production.

We estimate the amount of falsely b -tagged events (mistags) from the number of pretag W + light flavor events. The amount of pretag W + light flavor is determined by a fit of the pretag \cancel{E}_T distribution to W and non- W templates. To estimate the amount of W + light flavor in the tagged sample, we apply a per-jet false tag rate parameterization (mistag matrix) to the pretag W + light flavor events. The mistag matrix is obtained from inclusive jet data.

The number of events from W + heavy flavor is calculated using information from both data and Monte Carlo programs. We calculate the fraction of W events with associated heavy flavor production in the ALPGEN Monte Carlo program interfaced with the PYTHIA parton shower code [11, 12]. This fraction and the tagging efficiency

for such events are applied to the number of events in the original W +jets sample after correcting for the $t\bar{t}$ and electroweak contributions.

We use the \cancel{E}_T shape difference between the non- W and the other background models to constrain the amount of QCD events. We perform a likelihood fit to the \cancel{E}_T distribution to determine the total amount of QCD. We deduce the QCD fraction in the signal region by integrating the fitted distributions above our \cancel{E}_T cut (25 GeV for plug electrons, 10 GeV for the central muons, namely CMUP and CMX, and 20 GeV for all other leptons). We estimate the non- W contribution to the tagged sample by fitting the \cancel{E}_T distribution of the tagged events.

The summary of the background contributions is shown in Table II.

$WH \rightarrow \ell\nu b\bar{b}, 2\text{jets}$				
CDF Run II Preliminary 7.5 fb^{-1}				
Total	ST+ST	ST+JP	ST+NN	1-ST
Pretag Events	184050	184050	184050	184050
$t\bar{t}$	142 ± 22	114 ± 12	62.8 ± 6.4	479 ± 49
Single top(s-ch)	45.0 ± 6.7	35.1 ± 3.4	18.9 ± 1.8	106 ± 10
Single top(t-ch)	13.9 ± 2.4	13.3 ± 2.0	8.7 ± 1.2	191 ± 23
WW	1.67 ± 0.42	6.23 ± 2.08	5.14 ± 1.35	186 ± 25
WZ	12.9 ± 2.0	10.7 ± 1.2	5.84 ± 0.62	53.3 ± 6.2
ZZ	0.62 ± 0.09	0.49 ± 0.06	0.29 ± 0.03	2.05 ± 0.23
$Z + \text{jets}$	9.64 ± 1.40	11.9 ± 1.7	8.75 ± 1.30	182 ± 25
$Wb\bar{b}$	257 ± 104	228 ± 91	125 ± 50	1450 ± 580
$Wc\bar{c}/c$	31.0 ± 12.6	98.3 ± 40.5	63.8 ± 26.0	1761 ± 708
Mistag	12.1 ± 2.9	52.8 ± 15.2	57.0 ± 14.3	1646 ± 220
non- W QCD	57.9 ± 23.6	85.3 ± 34.1	74.9 ± 29.9	747 ± 299
Total background	584 ± 169	656 ± 194	432 ± 126	6802 ± 1822
Observed Events	519	568	402	6482
WH and ZH signal (115 GeV)	7.28 ± 0.98	5.34 ± 0.39	2.80 ± 0.19	16.0 ± 1.2

TABLE II: Background summary table for all the lepton categories combined.

IV. SYSTEMATIC UNCERTAINTIES

The b -tagging uncertainty is dominated by the uncertainty on the data/MC scale factors. The uncertainties due to initial- and final-state radiation are estimated by changing the parameters related to ISR and FSR, halving and doubling the default values. The difference from the nominal acceptance is taken as the systematic uncertainty. Other uncertainties on parton distribution functions, trigger efficiencies, or lepton identification contribute to a smaller extent to the overall uncertainty. Lepton reconstruction uncertainty is dominated by the variation of the data/MC scale factor for non-triggered muons and loose electron-like leptons. The effect of the uncertainty in the jet energy scale (JES) is evaluated by applying jet-energy corrections that describe $\pm 1\sigma$ variations to the default correction factor. The uncertainty in the shape of the BNN discriminant due to the JES is also taken into account. Also a shape systematic is considered for the uncertainty in the renormalization scale used to generate the $W + \text{jets}$ MC samples by halving and doubling the default value. A summary of the rate systematic uncertainties on the signal acceptance is given in Tables III, IV, V for the central electrons, forward electrons and non-triggered muons and loose electron-like leptons, respectively.

V. BAYESIAN NEURAL NETWORK

To improve further the signal to background discrimination after the event selection, we employ a Bayesian neural network trained on a variety of kinematic variables to distinguish WH events from the background. For this analysis, we employ distinct BNN discriminant functions that were optimized separately for the different tagging categories in order to increase the sensitivity. Each discriminant is optimized separately for each Higgs boson mass used in the search.

$WH \rightarrow \ell\nu bb$, 2jets						
CDF Run II Preliminary 7.5 fb ⁻¹						
b -tagging category	Lepton ID	Trigger	ISR/FSR/PDF	JES	b -tagging	Total
ST+ST	2%	< 1%	4.9%	2.0%	8.6%	10.3%
ST+JP	2%	< 1%	4.9%	2.8%	8.1%	10.1%
ST+NN	2%	< 1%	7.7%	2.2%	13.6%	15.9%
1-ST	2%	< 1%	3.0%	2.3%	4.3%	6.1%

TABLE III: Rate systematic uncertainties for central leptons.

$WH \rightarrow \ell\nu bb$, 2jets						
CDF Run II Preliminary 7.5 fb ⁻¹						
b -tagging category	Lepton ID	Trigger	ISR/FSR/PDF	JES	b -tagging	Total
ST+ST	2%	< 1%	7.7%	2.4%	8.6%	12.0%
ST+JP	2%	< 1%	4.5%	3.9%	8.1%	10.3%
ST+NN	2%	< 1%	12.9%	6.7%	13.6%	20.0%
1-ST	2%	< 1%	5.7%	2.9%	4.3%	8.0%

TABLE IV: Rate systematic uncertainties for forward electrons.

The discriminant used for the ST+ST tag category is trained using 7 input variables. The most sensitive is M_{jj} , which is the invariant mass calculated from the two tight jets. We correct this variable using a neural-network-based jet energy correction [13]. Another input variable is the p_T imbalance, which is the difference between the scalar sum of the p_T of all measured objects and the \cancel{E}_T . Specifically, it is calculated as $p_T(\text{jet}_1) + p_T(\text{jet}_2) + p_T(\text{lep}) - \cancel{E}_T$. The third variable is $M_{\ell\nu j}^{max}$, which is the invariant mass of the lepton, \cancel{E}_T , and one of the two jets, where the jet is chosen to give the maximum invariant mass. The fourth variable is $Q_{lep} \times \eta_{lep}$, the electric charge of the charged lepton times the η of the lepton. The fifth variable is the $\sum E_T$ (Loose Jets), which is the scalar sum of the loose jet transverse energy. A loose jet is defined as a jet having $|\eta| < 2.4$, $E_T > 12$ GeV and failing the nominal (tight) jet definition of $|\eta| < 2.0$, $E_T > 20$ GeV. The sixth variable is the $P_T(W)$, which is the transverse momentum of the reconstructed W , computed as $\vec{p}_T(\text{lep}) + \vec{p}_T(\nu)$. The seventh and last variable is H_T , which is the scalar sum of the transverse energies $H_T = \sum_{jets} E_T + p_T(\text{lep}) + \cancel{E}_T$.

The discriminant used for both the ST+JP and ST+NN tag category is trained with the same input variables as the ST+ST category, with the following exceptions. The variable $M_{\ell\nu j}^{max}$ is replaced by the variable $M_{\ell\nu j}^{min}$, which is the invariant mass of the lepton, \cancel{E}_T , and one of the two jets, where the jet is chosen to give the minimum invariant mass. The variable \cancel{E}_T , the missing transverse energy, replaces the variable p_T imbalance.

The discriminant used for the 1-ST tag category is trained with the same input variables as the ST+ST category, with the exception that the variable $M_{\ell\nu j}^{max}$ is replaced by the variable \cancel{E}_T and a new variable was added, namely $KITFlavorSeparator$, which is the output of an artificial-neural-network-based heavy flavor separator trained to distinguish b -quark jets from light flavor jets [14].

The training is defined such that the neural network attempts to produce an output as close to 1.0 as possible for

$WH \rightarrow \ell\nu bb$, 2jets						
CDF Run II Preliminary 7.5 fb ⁻¹						
b -tagging category	Lepton Reconstruction	Trigger	ISR/FSR/PDF	JES	b -tagging	Total
ST+ST	4.5%	3.0%	7.1%	1.7%	8.6%	12.5%
ST+JP	4.5%	3.0%	6.4%	2.4%	8.1%	11.9%
ST+NN	4.5%	3.0%	19.5%	1.9%	13.6%	24.5%
1-ST	4.5%	3.0%	8.4%	4.7%	4.3%	11.8%

TABLE V: Rate systematic uncertainties for non-triggered muons and loose electron-like leptons.

Higgs boson signal events and as close to 0.0 as possible for background events. Figure 1 shows a shape comparison of the BNN output between signal and background MC events for the ST+ST (top left), ST+JP (top right), ST+NN (bottom left) and 1-ST (bottom right) samples.

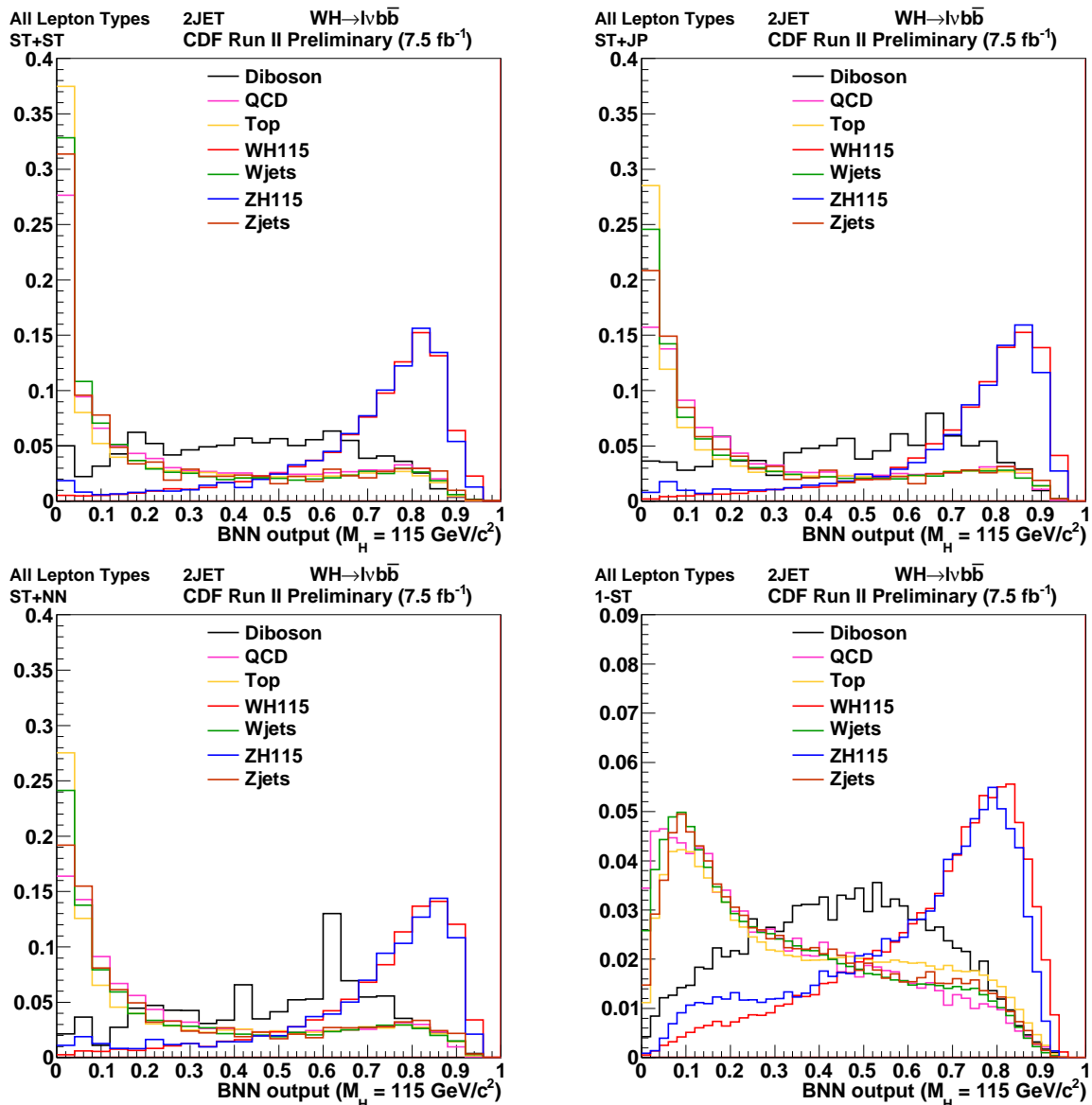


FIG. 1: Comparison of the BNN output for signal and background events. From left to right and top to bottom, ST+ST, ST+JP, ST+NN, and 1-ST, respectively. Signal and background histograms are each normalized to unit area. Central leptons, plug electrons, non-triggered muons, and loose electron-like leptons are combined.

VI. RESULTS

We perform a direct search for an excess in the signal region of the neural network output distribution from single-tagged and double-tagged $W+2$ jet events. A Bayesian statistical approach using a binned likelihood technique is used to estimate upper limits on Higgs boson production by constraining the number of background events to the estimates within uncertainties. For optimal sensitivity, the search is performed simultaneously in the separate ST+ST, the ST+JP, the ST+NN, and 1-ST categories.

Fig. 2 and Fig. 3 show the neural network output distributions for each b -tagging category. The data and predictions are in agreement within the uncertainties.

The combined expected and observed limits for all the lepton categories are shown in Figure 4 and Table VI. The expected and observed limits are also shown when the presented analysis is combined with the independent WH search for events with 3 jets, presented in [15].

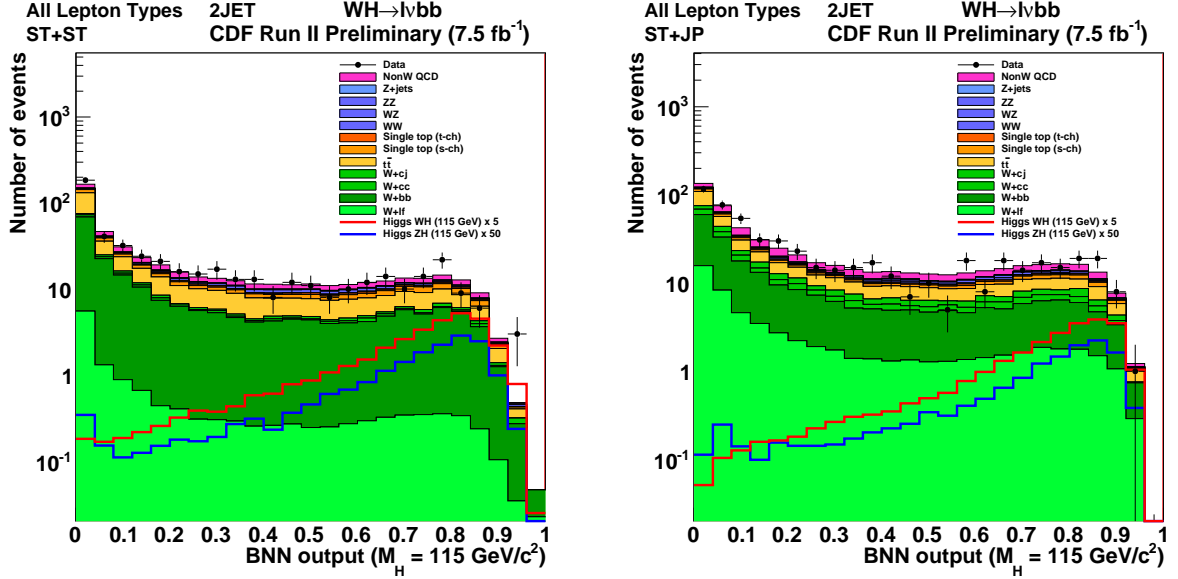


FIG. 2: Predicted and observed output for the neural network trained with a Higgs boson mass of $115 \text{ GeV}/c^2$ for ST+ST (left) and ST+JP (right). All lepton types are combined.

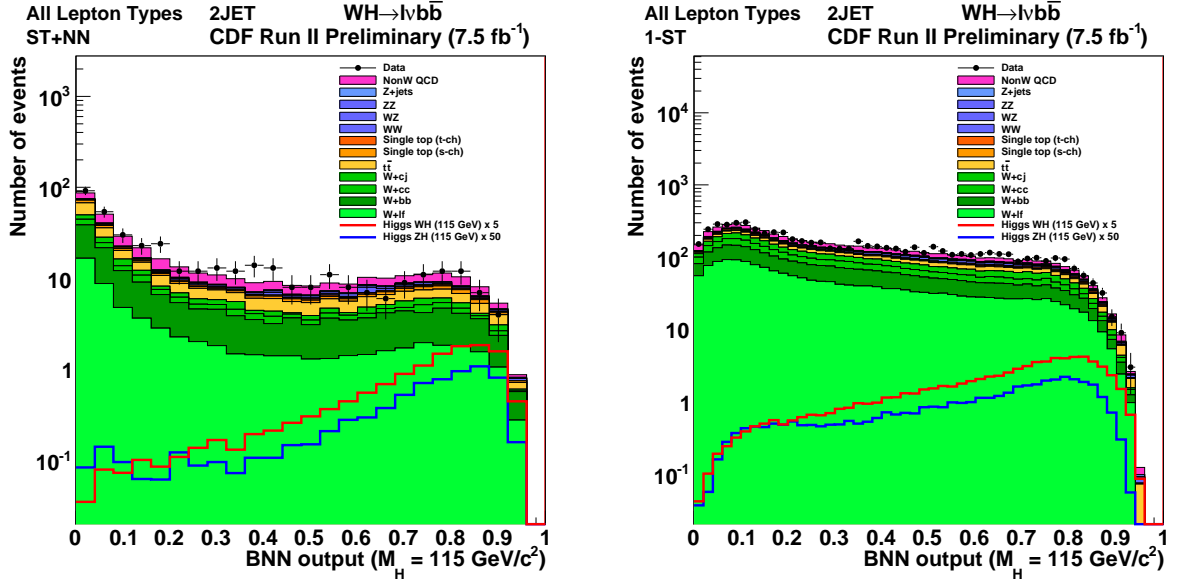


FIG. 3: Predicted and observed output for the neural network trained with a Higgs boson mass of $115 \text{ GeV}/c^2$ for ST+NN (left) and 1-ST (right). All lepton types are combined.

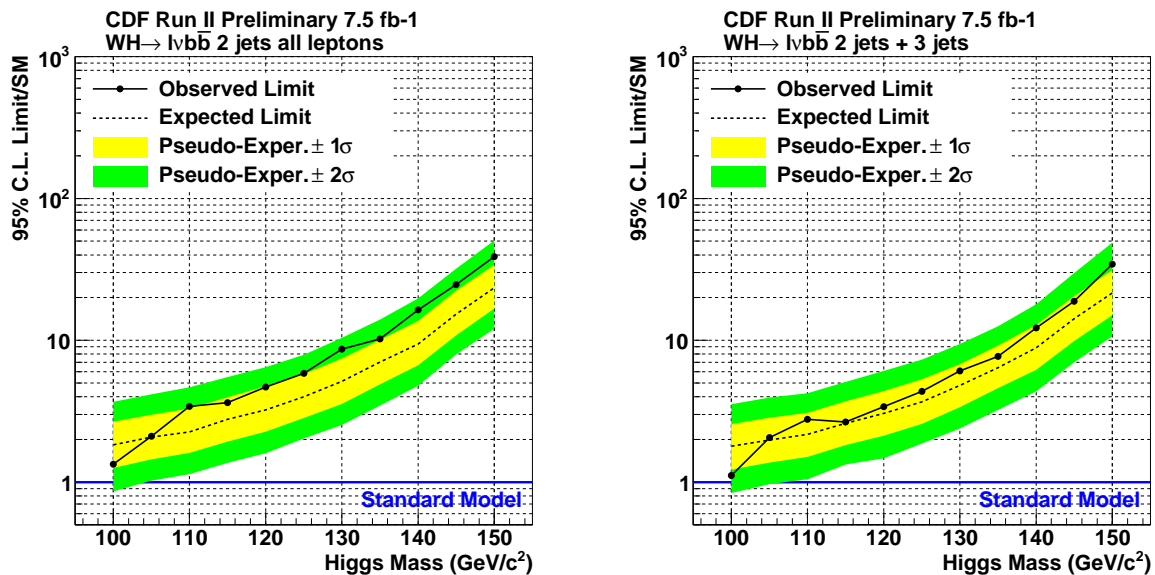


FIG. 4: Expected limits on Higgs boson production and decay for all lepton and tag categories combined, as a function of the Higgs boson mass hypothesis for the presented analysis (left) and after combining it with the independent search for events with 3 jets [15] (right). The plot shows the expected limit divided by the SM prediction for the Higgs boson cross section.

CDF Run II Preliminary 7.5 fb ⁻¹				
Limits for Combined Lepton and Tag Categories				
M(H) in GeV/c ²	2 jets		2 and 3 jets	
	Observed Limit	Expected Limit	Observed Limit	Expected Limit
100	1.34	1.83	1.12	1.79
105	2.10	2.08	2.06	1.98
110	3.42	2.26	2.78	2.17
115	3.64	2.78	2.65	2.60
120	4.68	3.22	3.40	3.06
125	5.84	4.01	4.36	3.69
130	8.65	5.13	6.09	4.80
135	10.2	7.02	7.71	6.40
140	16.4	9.39	12.3	8.84
145	24.7	15.3	18.9	14.2
150	38.8	23.4	34.4	21.6

TABLE VI: Observed and expected limits as a function of Higgs boson mass including all lepton and tag categories for the presented analysis and after combining it with the independent search for events with 3 jets [15].

VII. CONCLUSIONS

We have presented the results of a search for the standard model Higgs boson decaying to $b\bar{b}$, produced in association with a W boson decaying into a charged lepton and neutrino. We find that for the dataset corresponding to an integrated luminosity of 7.5 fb^{-1} , the data agree with the SM background predictions within the systematic uncertainties. We therefore set upper limits on the Higgs boson production cross section times the $b\bar{b}$ branching ratio. We find that the observed (expected) upper limits $\sigma(p\bar{p} \rightarrow W^\pm H) \times \text{Br}(H \rightarrow b\bar{b})$ range from $1.34 (1.83) \times \text{SM}$ to $38.8 (23.4) \times \text{SM}$ for masses ranging from $100 \text{ GeV}/c^2$ through $150 \text{ GeV}/c^2$. For $115 \text{ GeV}/c^2$ the upper limit is $3.64 (2.78)$. When we combine our analysis with an independent search using events with 3 jets [15], we set limits in the same mass range from $1.12 (1.79) \times \text{SM}$ through $34.4 (21.6) \times \text{SM}$ and for $115 \text{ GeV}/c^2$ the upper limit is $2.65 (2.60)$. The increase in sensitivity over the previous 5.7 fb^{-1} analysis [4] is 17% at $115 \text{ GeV}/c^2$, out of which 14.7% is due to the extra integrated luminosity and the rest due to improved analysis techniques.

Acknowledgments

We thank the Fermilab staff and the technical staffs of the participating institutions for their vital contributions. This work was supported by the U.S. Department of Energy and National Science Foundation; the Italian Istituto Nazionale di Fisica Nucleare; the Ministry of Education, Culture, Sports, Science and Technology of Japan; the Natural Sciences and Engineering Research Council of Canada; the National Science Council of the Republic of China; the Swiss National Science Foundation; the A.P. Sloan Foundation; the Bundesministerium für Bildung und Forschung, Germany; the Korean Science and Engineering Foundation and the Korean Research Foundation; the Science and Technology Facilities Council and the Royal Society, UK; the Institut National de Physique Nucleaire et Physique des Particules/CNRS; the Russian Foundation for Basic Research; the Ministerio de Educación y Ciencia and Programa Consolider-Ingenio 2010, Spain; the Slovak R&D Agency; and the Academy of Finland.

-
- [1] LEP Electroweak Working Group, <http://lepewwg.web.cern.ch/LEPEWWG/>
 - [2] ALEPH, DELPHI, L3, OPAL. The LEP Working Group for Higgs Boson Searches, Phys. Lett. B **565** 61 (2003).
 - [3] T. Han and S. Willenbrock, Phys. Lett. **B273** (1991) 167;
A. Djouadi, J. Kalinowski, and M. Spira, Comp. Phys. Commun. **108 C** (1998) 56.
 - [4] T. Aaltonen *et al.* (CDF Collaboration), CDF Public Note 10239 (2010).
 - [5] <http://www.cs.utoronto.ca/~radford/fbm.software.html>
 - [6] C. C. Chang and C. J. Lin, LIBSVM: a library for support vector machines.
 - [7] F. Abe *et al.*, Nucl. Instrum. Methods Phys. Res. A **271**, 387 (1988);
D. Amidei *et al.*, Nucl. Instrum. Methods Phys. Res. A **350**, 73 (1994);
F. Abe *et al.*, Phys. Rev. D **52**, 4784 (1995);
P. Azzi *et al.*, Nucl. Instrum. Methods Phys. Res. A **360**, 137 (1995);
The CDF II Detector Technical Design Report, Fermilab-Pub-96/390-E.
 - [8] B. Casal, FERMILAB-THESIS-2009-21 (2009).
 - [9] A. Abulencia *et al.*, Phys. Rev. **D71**, 072005 (2005).
 - [10] D. Buskulic *et al.* (ALEPH Collaboration), Phys. Lett. B **313**, 535 (1993);
F. Abe *et al.* (CDF Collaboration), Phys. Rev. D **53**, 1051 (1996);
A. Affolder *et al.* (CDF Collaboration), Phys. Rev. D **64**, 032002 (2001), Erratum-ibid: Phys. Rev. D **67**, 119901 (2003).
 - [11] P. Edén, C. Friberg, L. Lönnblad, G. Miu, S. Mrenna, E. Norrbin, and T. Sjöstrand, Computer Phys. Commun. **135** (2001) 238.
 - [12] M.L. Mangano *et al.*, JHEP 0307:001, 2003.
 - [13] T. Aaltonen *et al.*, Improved b -jet Energy Correction for $H \rightarrow b\bar{b}$ Searches at CDF, arXiv:1107.3026 (2011).
 - [14] S. Richter, FERMILAB-THESIS-2007-35 (2009).
 - [15] T. Aaltonen *et al.* (CDF Collaboration), CDF Public Note 10217 (2011).